Electronic Supplementary Material (ESI) for Physical Chemistry Chemical Physics.

Supplementary Information: Insight into the Chromophore of Rhodopsin and its Meta-II Photointermediate by ^{19}F Solid-State NMR and Chemical Shift Tensor Calculations

Andreas Brinkmann[a,], Ulrich Sternberg[b], Petra H. M. Bovee-Geurts[c], Isabelle Fernández Fernández[d,f], Johan Lugtenburg[d], Arno P. M. Kentgens[e] and Willem J. DeGrip[c,d,]**

[a] Metrology, National Research Council Canada, 1200 Montreal Road, Ottawa, Ontario, K1A 0R6, Canada

[b] Karlsruhe Institute of Technology, P. O. Box 3640, 76021 Karlsruhe, Germany

[c] Department of Biochemistry, UMCN 286, Radboud Institute for Molecular Life Sciences, Radboud University Medical Center, P.O. Box 9101, 6500 HB Nijmegen, The Netherlands

[d] Leiden Institute of Chemistry, Leiden University, P.O. Box 9502, 2300 RA Leiden, The Netherlands

[e] Institute for Molecules and Materials, Radboud University Nijmegen, Heyendaalsweg 135, 6525 AJ Nijmegen, The Netherlands

[f] Present address: International Flavors & Fragrances, Avda. Felipe Klein 2, 12580 Benicarló (Castellon), Spain

*Corresponding authors:

E-mail: Andreas.Brinkmann@nrc-cnrc.gc.ca

E-mail: Wim.deGrip@radboudumc.nl

NMR Modeling and Chemical Shift Tensor Calculation of the Retinal System

S.1. NMR calculations and modeling for the dark adapted structure

S.1.1 Modeling Protocol

Structure: T. Okada *et al.* (1) Crystal Structure of Rhodopsin at 2.2Å (1U19.pdb)

1. All molecules of unit A are extracted and stored as coordinate file A_1U19.coo (COSMOS-NMR).

2. Bond types of the protein part are corrected. The X-ray method does not give correct bond lengths for some groups. The bond types are needed in force field calculations.

3. Palmitoyl groups are not taken into account, see Okada *et al.* (1).

4. The Hg^{2+} and Zn^{2+} are substituted by water molecules. The same procedure was used by Okada et al.

5. Charged groups are assigned to the protein part. Two versions are created: (i) Glu 181 and Glu 122 are protonated and treated as uncharged, see Fahmy *et al.* (2) and Yan *et al.* (3) and a second version (ii) where Glu 181 is charged.

6. Hydrogen atoms are added and subjected to a short geometry optimization to avoid close Van der Waals contacts.

7. Hydrogen bridges of the protein backbone are introduced as distance constrains to preserve the general structure in MD simulations and global minima search.

8. To heal out Van der Waals contacts from the automatic hydrogen generation the molecular model was annealed from 10K to 300K and 1053 coordinate files were saved as MD snapshots. During this process 317 backbone N-H...O-C hydrogen bonds were used as constrains to preserve the overall structure of the protein.

9. For geometry optimization with ^{13}C chemical shifts the data of Frähmcke *et al.* (4) are used (see Table 5, column exp. Rh^{c}), which are the average of the results reported in Refs. (5,6,7,8,9,10,11).

10. The 1053 structures are geometry optimized with the ^{13}C chemical shifts as constraints (12). The atomic charges and ^{13}C chemical shifts were calculated at every step of the geometry optimization (conjugated gradient method).

11. From the 1053 structures the 20 with the lowest pseudo-energy were selected. These 20 structures are used in all further investigations.

12. The hydrogen atom H12 was replaced by a fluorine atom (F12) and the 20 fluorinated structures were geometry optimized. This free geometry optimization (without constraints) will change only the next surrounding of the fluorine atom.

13. The 20 structures were geometry optimized with the isotropic ^{19}F chemical shifts of F12 (δ=-95.0 ppm/$CFCl_3$) as constraints. In this process the ^{19}F chemical shift tensor of the F12 was calculated (BPT parameter file: cs19f_tzvpp_mp2_ns_ref.pol).

S.1.2 Results for the dark state (rhodopsin)

S.1.2.1 ^{13}C CS optimized backbone structure

We have to keep in mind that the ^{13}C chemical shifts are obtained from molecules that are embedded within the membrane bilayer with its 7 membrane spanning helices. To preserve the global features of the protein part of the X-ray structure the hydrogen bridges of the backbone were used as additional constraints. Because no long range distance constrains are introduced some parts of the molecule shifted from its original position. The loop regions changed most but these regions

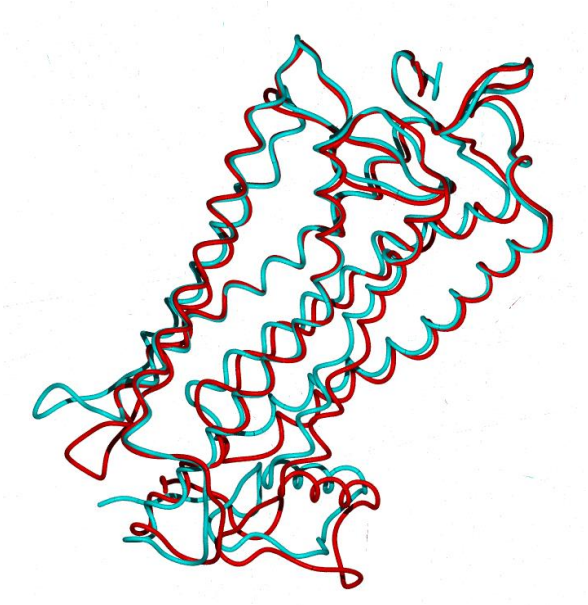

Figure S1: Overlay of the original structure of rhodopsin (1U19; turquoise) with a CS optimized structure with ^{13}C chemical shifts of retinal and backbone hydrogen bridges as constraints (red). Only the protein backbone is displayed.

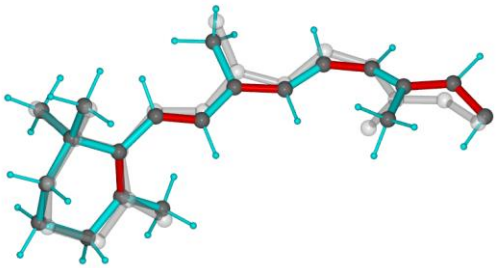

Figure S2a: RMS overlay of the retinal backbone of the X-ray structure (grey) with the CS optimized structure (blue).

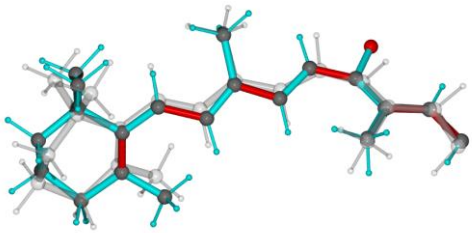

Figure S2b: Overlay of the best ^{13}C CS optimized structure (in gray) with the best ^{19}F CS optimized structure (blue).

are supposed to be flexible in the membrane bound state. The RMS deviation of the distance constraints for the backbone hydrogen bridges was 0.2 Å and this deviation indicates how well the general features of the structure are reserved (Fig. S1).

S.1.2.2 ^{13}C CS optimized retinal structure

In the following we use the term "best structure" for the one with the lowest CS pseudo-energy and consequently the lowest RMS deviation between calculated and experimental chemical shifts.

The overlay of the backbone of the X-ray structure of retinal (Figure S2a) with the CS optimized structure gave a RMS deviation of 0.39 Å conserving all features of the X-ray structure for the best structure.

If hydrogen 12 is substituted with fluorine the optimization with the ^{19}F CS yields the number 18 of the ^{13}C CS optimized structures as best structure (see Figure S2b). The RMS deviation to the structure number 1 is 0.67Å. This deviation is caused by the slightly other conformation of the 6 membered ring. The difference of the structures is not primarily caused by the optimization but mostly by the selection of another structure that fits better to the ^{19}F isotropic CS.

Inspecting all 20 models (section S.1.1 step 11) some different conformers of the retinal showed up. 15 out of the 20 best structures, including the best structure, retained the original conformation of the retinal (Figure S3 top). Two structures display a slightly different orientation of the 6 membered ring (Fig. S3, bottom). In three structures (Fig. S3, middle) the retinal backbone conformation was changed. In 17 of 20 structures the torsion angle C9-C10-C11-C12 is *cis* (values between -24.5° to 6.5°, -25.5 for the best model) whereas this angle flips to *trans* (values between 168 to -170°) in

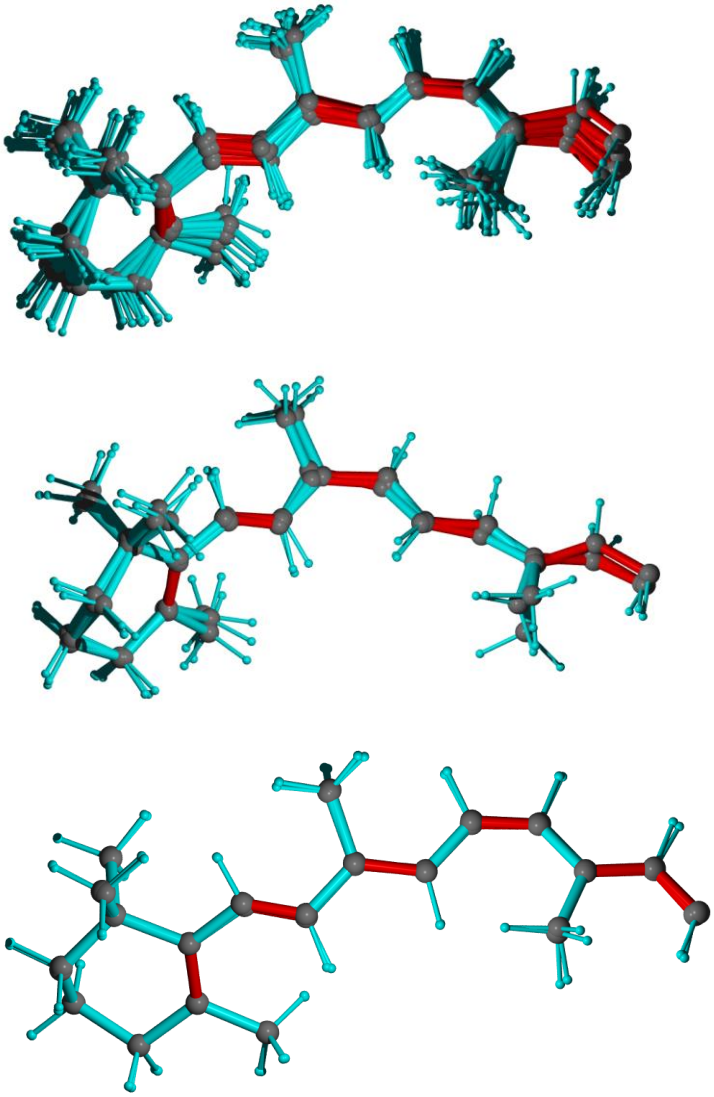

Figure S3: Retinal conformers that appeared within the 20 best ^{13}C CS optimized structures of the dark adapted form (rhodopsin).

The coloring of the bonds only indicates that there is an alternating π-bond length. For further explanation see text.

these 3 structures (Fig. S3, middle). This retinal conformation occurs also in isorhodopsin that was investigated by Nakamichi *et al.* (13,14). Their X-ray structure contains two Retinals in the asymmetric unit with C10-C11-C12-C13 torsion angles of 166.9° and 166.4°. The coloring of the bonds should only indicate that there is an alternating π-bond length. Since the ^{13}C chemical shift strongly depends on the valence of the π-bonds, this parameter will be adjusted in the course of the geometry optimization.

The resulting ^{13}C chemical shifts for the best structure are compared with the experimental values in Table S1.

Table S1: Calculated and experimental ^{13}C chemical shifts of retinal in rhodopsin (11-*cis*)

Carbon site	^{13}C CS Exp. [1)] /ppm TMS	^{13}C CS BPT /ppm TMS	^{13}C CS BPT /ppm referenced	Difference[2)] / ppm
C1_RET	34	34.276	36,145	2,145
C2_RET	40	34.944	36,813	-3,187
C3_RET	20	31.47	-	-
C4_RET	34	33.988	35,857	1,857
C5_RET	130	129.721	131,59	1,59
C6_RET	137	134.114	135,983	-1,017
C7_RET	132	130.115	131,984	-0,016
C8_RET	139	137.206	139,075	0,075
C9_RET	148	146.513	148,382	0,382
C10_RET	127	127.596	129,465	2,465
C11_RET	141	137.173	139,042	-1,958
C12_RET	132	130.481	132,35	0,35
C13_RET	168	164.25	166,119	-1,881
C14_RET	121	116.062	117,931	-3,069
C15_RET	165	162.14	164,009	-0,991
C16_RET	30	24.637	26,506	-3,494
C17_RET	26	24.902	26,771	0,771
C18_RET	21	21.023	22,892	1,892
C19_RET	13	13.483	15,352	2,352
C20_RET	16	15.865	17,734	1,734

[1)] Data taken from Frähmke *et al.* (4), which are the average of the results reported in Refs. (5,6,7,8,9,10,11).

[2)] RMSD without C3: 1.93 ppm

The largest deviation with 11.5 ppm comes from sp^3 ring carbon atom C3 (Table S2). The RMS deviation of calculated and measured ^{13}C chemical shifts including this carbon is 3.6 ppm. Upon eliminating this largest difference it is observed that on average the calculated values are by 1.869 ppm too small. Since this difference may be caused by the theoretical reference or by an experimental reference shift it is recommended to re-reference the values using the mean as

Table S2: Calculated ^{19}F principal tensor elements of F12 in comparison to the experimental values

Tensor component	Experimental values / ppm $CFCl_3$	Calculated values uncorrected	/ ppm $CFCl_3$ corrected for Δ-isotropic shift
11	-41.7	-54.0	-34.8
22	-99.9	-124.0	-104.8
33	-143.4	-164.1	-144.9

reference. The RMS deviation of the re-referenced values is 1.93 ppm. The reason for the large deviation of C3 may originate in the existence of other ring conformers of the 6 membered ring. For instance, the torsion angle C1-C2-C3-C4 for the best dark model is 62° and in the light adapted structure this angle has flipped to -64°.

S1.2.3 ^{19}F CS optimized retinal structure in the dark state (rhodopsin)

The calculations reveal a large deviations of the isotropic ^{19}F shifts in comparison to the experimental value (-95.0 ppm / $CFCl_3$). The calculated value of the best structure is with -114.2 ppm by 19.2 ppm too small. If we shift all calculated tensor values by 19.2 ppm we obtain tensor values that compare well with the experiment (Table S2).

The next non bonded neighbor of the fluorine is Hα1 of glycine 114 with a distance of 1.768Å (Fig. S4a). This short contact resembles a hydrogen bridge and will have large influence on the fluorine

Table S3: Calculated ^{19}F principal tensor elements of F12 for deprotonated Glu-181 in comparison to the experiment. All calculated values are shifted by 15.6 ppm to the experimental isotropic value.

Tensor component	Experimental value / ppm $CFCl_3$	Calculated values uncorrected	/ ppm $CFCl_3$ corrected for Δ-isotropic shift
11	-41.7	-47.3	-31.7
22	-99.9	-126.7	-111.1
33	-143.4	-157.8	-142.2

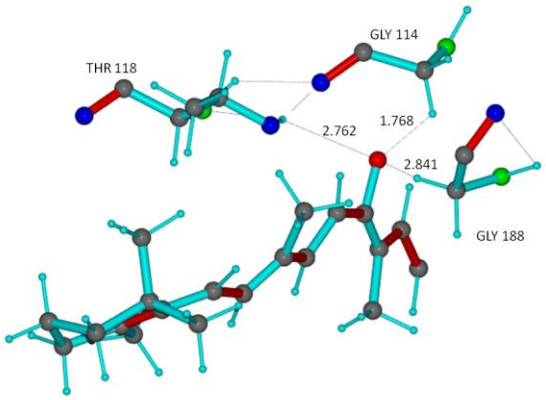

Figure S4a: Short contacts of fluorine to hydrogens of the protein binding pocket in the best structure.

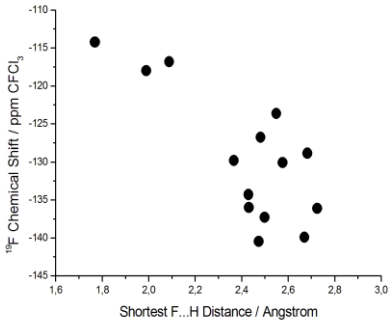

Figure S4b: Isotropic ^{19}F CS depends on shor distance between the fluorine and hydrogens binding pocket in a family of structures.

chemical shift. The model with the shortest contact has the smallest difference to the experimental isotropic CS value. There is a clear tendency that the calculated isotropic CS gets larger negative values with growing distance of the shortest F...H contact (Fig. S4b). The 5th best model has a shortest distance of 2.481 to Hß3 of ALA 117 and an isotropic CS value of -126.76 ppm. An important contribution to the ligation shift in comparison with the similar compound in solution therefore lies in short F...H contacts to partial positive hydrogen atoms of the protein backbone or side chains, mainly Hα1 of glycine 114, and188, Hß of alanine 117 and Hɣ of threonine 118.

It is not surprising that the span of the experimental tensor is somewhat smaller than that of the calculated tensor (Table S2), since even at 200K there is always a narrowing of the static tensor by internal motions.

S1.2.4 The Effect of the Protonation of Glu 181 on the ^{19}F CS

The proton was removed from the COOH-group of Glutamate 181 and this group was treated as a carboxylate (COO^-) group. This was done for the 20 best structures. These molecules were now optimized with the experimental isotropic ^{19}F chemical shift as constraint. The resulting best isotropic shift was with -110.6 ppm (experiment -95.0 ppm) slightly better than in the case of the protonated Glu 181 (-114.2 ppm). The corresponding tensor elements are presented in Table S3.

The surrounding of the fluorine was similar with Glu-181 protonated or deprotonated. When corrected for the difference in isotropic CS the calculated tensor element values in Table S3

correspond quite well with the experimental ones, but are less close then when Glu-181 is protonated (Table S2).

S2. NMR calculations and modeling for the light activated structure (Meta II)

S2.1 Modeling Protocol

Structure: X. Deupi *et al.* (15) (PDB ID 4A4M)

1. All molecules of the asymmetric unit that were given in the PDB file 4A4M are extracted and stored as coordinate file A_4A4M.coo (COSMOS-NMR). The structure consisted of the metarhodopsin-II in complex with G protein alpha subunit (GαCT).

2. The single and conjugated double bond types of the protein and GαCT are corrected. The X-ray method does not give bond lengths precise enough for automated bond search. The correct single and double bonds are needed for force field calculations.

3. Hydrogen atoms are added and subjected to a short geometry optimization to avoid close Van der Waals contacts. The main source of these Van der Waals contacts are water oxygen atoms and the orientation of the water hydrogen atoms is selected at random.

4. Charged groups are assigned to the protein and the GαCT part of the system.

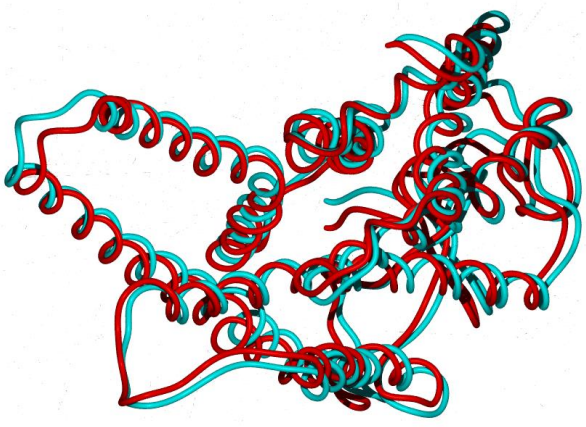

Figure S5: Overlay of the original structure 4A4M (turquoise) with a CS optimized structure with ^{13}C chemical shifts of retinal and backbone hydrogen bridges as constraints (red). Only the protein backbone is displayed.

5. Hydrogen bridges of the protein and GαCT backbone are introduced as distance constrains to preserve the general structure in MD simulations and global minima search.

6. To heal out VdW contacts from the automatic hydrogen generation the molecular model was annealed from 10K to 300K and 1053 coordinate files were saved as MD snapshots. During this process 317 backbone N-H...O-C hydrogen bonds were used as constrains to preserve the overall structure of the protein.

7. All 1053 snapshots are geometry optimized using the COSMOS-NMR force field. The backbone hydrogen bond distances are used as constraints to avoid larger distortion of the original structure.

8. The 1053 structures are geometry optimized with ^{13}C chemical shifts of the Retinal part to generate structures that display a surrounding of the active site that resembles as close as possible the conditions that are present in the NMR investigations. For geometry optimization with ^{13}C chemical shifts the data of Smith *et al.* (16) (also see Frähmcke *et al.* (4) Table 5, column exp. Rh^{d}) are used.

The atomic charges and ^{13}C chemical shifts were calculated at every step of the geometry optimization (conjugated gradient method) (12).

9. From the 1053 structures the 20 with the lowest pseudo-energy were selected. These 20 structures are used in all further investigations.

10. The 20 best structures were geometry optimized with the isotropic ^{19}F constraint (-130.0 ppm $CFCl_3$) to adjust the surrounding of the fluorine to experimental conditions. In this process the ^{19}F chemical shift tensor of the F12 was calculated (BPT parameter file: cs19f_tzvpp_mp2_ns_ref.pol).

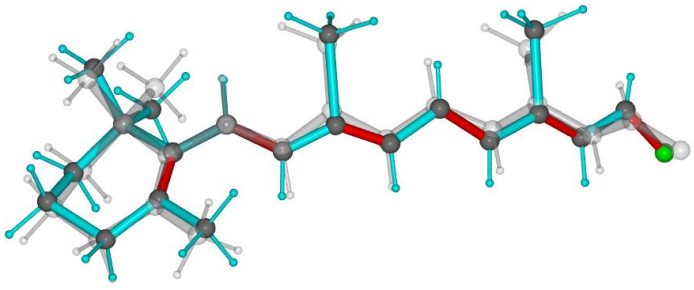

Figure S6: RMS overlay of the atoms of retinal in Meta II of the X-ray structure (grey) with the ^{13}C CS optimized structure (blue).

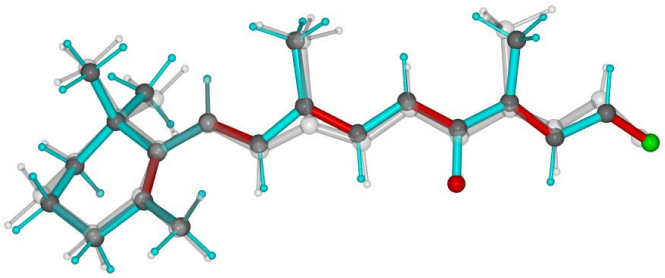

Figure S7: RMS overlay of the atoms of retinal of the ^{13}C CS optimized structure (grey) with the ^{19}F CS optimized structure (blue)..

S2.2 Results for the light adapted structure (Meta II)

S2.2.1 ^{13}C CS optimized backbone structure

Comparing the original backbone structure with the best ^{13}C chemical shift optimized structure (Fig. S5) we state that all general features of the protein are conserved. The 314 backbone hydrogen bonds were used as distance constraints in the MD simulation and in the first geometry optimization without chemical shifts. The RMS deviation of the distance constraints for the backbone hydrogen bridges was 0.21 Å. When we do not count shorter distances (they do not violate constraints) we arrive at an RMS deviation of only 0.08 Å.

S2.2.2 ^{13}C CS optimized retinal structure

The X-ray structure and the ^{13}C CS optimized structure of the retinal in Meta II are very similar and the RMS deviation is only 0.43 Å (see Figure S6).

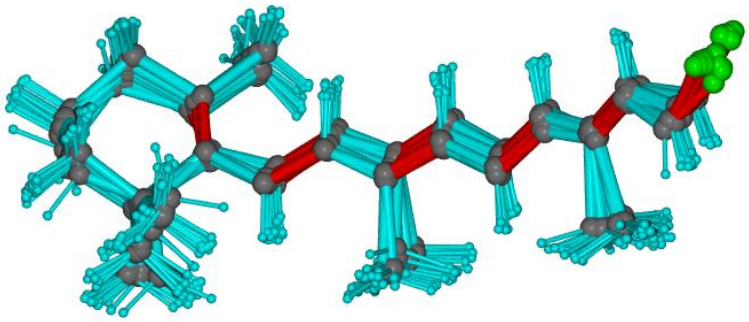

Figure S8: RMS overlay of the 20 best ^{13}C optimized retinal structures in Meta II.

In the case of the ^{19}F optimized structure (Fig. S7) only small changes are observed and these changes are mainly due to selection of the 13th best ^{13}C optimized structure. The RMS deviation of the heavy atoms (excluding fluorine) is only 0.26Å.

Table S4: Calculated and experimental ^{13}C chemical shifts of retinal in Meta II.

Carbon site	^{13}C CS Exp.[1)] /ppm TMS	^{13}C CS BPT /ppm referenced	Difference [2)] /ppm
C1_RET_A_401	34	35.44	1.44
C2_RET_A_401	42	34.71	-7.29
C3_RET_A_401	18	26.45	8.45
C4_RET_A_401	34	35.03	1.03
C5_RET_A_401	144	142.96	-1.04
C6_RET_A_401	135	134.26	-0.74
C7_RET_A_401	129	128.48	-0.52
C8_RET_A_401	132	130.23	-1.77
C9_RET_A_401	146	144.26	-1.74
C10_RET_A_401	133	132.09	-0.91
C11_RET_A_401	139	138.91	-0.09
C12_RET_A_401	134	131.76	-2.24
C13_RET_A_401	164	165.70	1.70
C14_RET_A_401	122	123.18	1.18
C15_RET_A_401	160	152.22	-7.78
C16_RET_A_401	28	27.44	-0.56
C17_RET_A_401	28	28.68	0.68
C18_RET_A_401	22	23.43	1.43
C19_RET_A_401	11	10.92	-0.07
C20_RET_A_401	13	14.07	1.07

[1)] Data taken from Frähmke *et al.* (4)

[2)] ^{13}C - RMSD = 3.243 ppm referenced for all retinal carbon values. The ^{13}C - RMSD = 2.808 ppm when referenced and eliminating the maximum deviation of carbon 15 of -7.78 ppm

Table S5: Calculated ^{19}F principal tensor elements of F12 in comparison to the experiment.

Tensor component	Experimental value / ppm $CFCl_3$	Calculated value / ppm ref. isotropic value
11	-76.8	-70.5
22	-130.9	-118.5
33	-185.0	-187.7

All 20 best ^{13}C optimized structures of retinal in Meta II are similar and no other conformers appeared in the MD simulation (Fig. S8). As already mentioned not only the retinal backbone is different from the dark state model rhodopsin but also the 6 membered ring has another conformation. The torsion angle C1-C2-C3-C4 for the best model is -64° (compared to 62° for the dark state structure).

The calculated ^{13}C chemical shifts of the best Meta II structure are tabulated in Table S4, and compared to the experimental values.

Large CS deviations are observed for the CH_2 groups of the 6 membered ring (C2 and C3) as in the case of the dark adapted structure. A large deviation however appears also for the carbon C15 connecting the retinal to the protein backbone by a bond to nitrogen. Since we have no constraints on the nitrogen the surrounding of C15 is a weaker constraint than the other carbons. This carbon atom was therefore excluded for the calculation of the mean reference. The CS RMS deviation excluding C15 is 2.8 ppm

S2.2.3 ^{19}F CS optimized retinal structure in Meta II

The calculated isotropic ^{19}F shifts for the best Meta II model fit much better to the experimental value (-130.9 ppm / $CFCl_3$) than in the case of the dark state model. The calculated value of the best structure is with -125.6 ppm by 5.3 ppm too large. If we shift all calculated tensor values by 5.3 ppm we obtain tensor values that compare well with the experimental values (Table S5).

The fluorine in the best structure has close contacts to H_N of isoleucine 189 (2.410Å) and to Hε2 of tyrosine 286 (2.621Å, proton on the aromatic ring). The effect of these closest residues on the bond polarization cancel each other to a large extent, resulting in a significant decrease of the chemical shift.

References

1. Okada T, Sugihara M, Bondar AN, Elstner M, Entel P, Buss V. The retinal conformation and its environment in rhodopsin in light of a new 2.2 Å crystal structure. J. Mol. Biol. 2004; 342(2): p. 571-583.
2. Fahmy K, Jäger F, Beck M, Zvyaga TA, Sakmar TP, Siebert F. Protonation states of membrane-embedded carboxylic acid groups in rhodopsin and metarhodopsin II: a Fourier-transform infrared spectroscopy study of site-directed mutants. Proc. Natl. Acad. Sci. U. S. A. 1993; 90(21): p. 10206-10210.
3. Yan ECY, Kazmi MA, De S, Chang BSW, Seibert C, Marin EP, et al. Function of extracellular loop 2 in rhodopsin: Glutamic acid 181 modulates stability and absorption wavelength of metarhodopsin II. Biochemistry. 2001; 41(11): p. 3620-3627.
4. Frähmcke JS, Wanko M, Phatak P, Mroginski MA, Elstner M. The protonation state of Glu181 in rhodopsin revisited: Interpretation of experimental data on the basis of QM/MM calculations. J. Phys. Chem. B. 2010; 114(34): p. 11338-11352.
5. Verhoeven MA, Creemers AFL, Bovee-Geurts PHM, DeGrip WJ, Lugtenburg J, de Groot HJM. Ultra-high-field MAS NMR assay of a multispin labeled ligand bound to its G-protein receptor target in the natural membrane environment: Electronic structure of the retinylidene chromophore in rhodopsin. Biochemistry. 2001; 40(11): p. 3282-3288.
6. Creemers AFL, Kiihne SR, Bovee-Geurts PHM, DeGrip WJ, Lugtenburg J, de Groot HJM. ^{1}H and ^{13}C MAS NMR evidence for pronounced ligand-protein interactions involving the ionone ring of the retinylidene chromophore in rhodopsin. Proc. Natl. Acad. Sci. U. S. A. 2002; 99(14): p. 9101-9106.
7. Smith SO, Palings I, Miley ME, Courtin J, De Groot H, Lugtenburg J, et al. Solid-state NMR studies on the mechanism of the opsin shift in the visual pigment rhodopsin. Biochemistry. 1990; 29(35): p. 8158-8164.
8. Smith SO, Courtin J, De Groot H, Gebhard R, Lugtenburg J. ^{13}C magic-angle spinning NMR studies of bathorhodopsin, the primary photoproduct of rhodopsin. Biochemistry. 1991; 30(30): p. 7409-7415.
9. Mollevanger LCPJ, Kentgens APM, Pardoen JA, Courtin JML, Veeman WS, Lugtenburg J, et al. High-resolution solid-state ^{13}C-NMR study of carbons C-5 and C-12 of the chromophore of

bovine rhodopsin: Evidence for a 6-*S*-*cis* conformation with negative-charge perturbation near C-12. Eur. J. Biochem. 1987; 163(1): p. 9-14.

10. Spooner PJR, Sharples JM, Verhoeven MA, Lugtenburg J, Glaubitz C, Watts A. Relative Orientation between the β-Ionone Ring and the Polyene Chain for the Chromophore of Rhodopsin in Native Membranes. Biochemistry. 2002; 41(24): p. 7549-7555.
11. Concistrè M, Gansmüller A, McLean N, Johannessen OG, Montesinos IM, Bovee-Geurts PHM, et al. Double-quantum ^{13}C nuclear magnetic resonance of bathorhodopsin, the first photointermediate in mammalian vision. J. Am. Chem. Soc. 2008; 130(32): p. 10490-10491.
12. Jakovkin I, Klipfel M, Muhle-Goll C, Ulrich AS, Luy B, Sternberg U. Rapid calculation of protein chemical shifts using bond polarization theory and its application to protein structure refinement. Phys. Chem. Chem. Phys. 2012; 14(35): p. 12263-12276.
13. Nakamichi H, Okada T. X-ray crystallographic analysis of 9-*cis*-rhodopsin, a model analogue visual pigment. Photochem. Photobiol. 2007; 83(2): p. 232-235.
14. Nakamichi H, Buss V, Okada T. Photoisomerization mechanism of rhodopsin and 9-*cis*-rhodopsin revealed by X-ray crystallography. Biophys J. 2007; 92(12): p. L106–L108.
15. Deupi X, Edwards P, Singhal A, Nickle B, Oprian D, Schertler G, et al. Stabilized G protein binding site in the structure of constitutively active metarhodopsin-II. Proc. Natl. Acad. Sci. U. S. A. 2012; 109(1): p. 119-124.
16. Smith SO, De Groot HJM, Gebhard R, Courtin JML, Lugtenburg J, Herzfeld J, et al. Structure and protein environment of the retinal chromophore in light- and dark-adapted bacteriorhodopsin studied by solid-state NMR. Biochemistry. 1989; 28(22): p. 8897-8904.